Commun. Theor. Phys. (Beijing, China) **53** (2010) pp. 913–919

Vol. 53, No. 5, May 15, 2010

Apparently Negative Electric Polarization in Shaped Graded Dielectric Materials*

FAN Chun-Zhen (范春珍),[1] GAO Yin-Hao (高银浩),[2] GAO Yong (高勇),[1] and HUANG Ji-Ping (黄吉平)[1,†]

[1]Surface Physics Laboratory (National Key Laboratory) and Department of Physics, Fudan University, Shanghai 200433, China

[2]School of Machinery and Electricity, Henan Institute of Science and Technology, Xinxiang 453003, China

(Received July 27, 2009; revised manuscript received October 23, 2009)

Abstract *By using a first-principles approach, we investigate the pathway of electric displacement fields in shaped graded dielectric materials existing in the form of cloaks with various shapes. We reveal a type of apparently negative electric polarization (ANEP), which is due to a symmetric oscillation of the paired electric permittivities, satisfying a sum rule. The ANEP does not occur for a spherical cloak, but appears up to maximum as a/b (the ratio between the long and short principal axis of the spheroidal cloak) is about 5/2, and eventually disappears as a/b becomes large enough corresponding to a rod-like shape. Further, the cloaking efficiency is calculated for different geometrical shapes and demonstrated to closely relate to the ANEP. The possibility of experiments is discussed. This work has relevance to dielectric shielding based on shaped graded dielectric materials.*

PACS numbers: 41.20.-q, 05.70.Fh
Key words: shaped graded materials, negative electric polarization, electric displacement fields

1 Introduction

Metamaterials[1−2] are a class of electromagnetic materials, which are currently under extensive investigation.[3−15] They owe their properties to subwavelength details of structure rather than to their chemical composition, and can be designed to have properties difficult or impossible to find in nature. One outstanding case of the metamaterials is the realization of electromagnetic cloaks, which was put forth by Pendry *et al.*[3] It is well-known for hiding objects from electro-magnetic waves,[4−5,9] due to the high freedom of design of metamaterials,[6] which may be both inhomogeneous and anisotropic in their electric permittivity and magnetic permeability.[3−7] Owing to intriguing potential applications, it has received extensive attention both theoretically and experimentally.

For a spherical cloak, the obtained permittivities are anisotropic along the three directions in spherical coordinates. However, to simplify the material parameters we may focus on two dimensional cases. As for a cylindrical cloak, which was first experimentally demonstrated[5] and theoretically studied at optical frequencies.[9] The cross section[7] for the two dimensional cylindrical invisibility cloak was explored. It has been conjectured that, in the quasistatic regime, dielectric bodies of finite size could be perfectly cloaked by certain cylindrical arrangements of materials of positive and negative permittivities known as superlenses.[16] Meanwhile the elliptic electromagnetic cloaks have been studied,[17−19] where the required material properties of the cloak were derived in terms of the geometrical parameters and the coordinates in the transformed system.[19]

Now, the interest in the study of the cloak has been extended to acoustic cloaks,[11,20−22] elastic cloaks,[23] and thermal cloaks.[25] The realization of acoustic cloaks depends on the elastic transformation medium, which should show radius-dependent distributions for anisotropic density and bulk modulus.[24] The apparently negative thermal conductivity of the thermal cloak has already been studied.[25]

In this work, by using a first-principles approach based on the coordinate transformation method, we shall investigate cloaks made of graded dielectric materials, and clarify their universality concerning apparently negative electric polarization (ANEP) as geometric shapes of the cloak change in a typical range. We shall further calculate the cloaking efficiency of the cloaks with various shapes, which is shown to be closely related to the ANEP.

The remainder of this work is organized as follows. In Sec. 2, based on the coordinate transformation method, we present a first-principles approach to derive the expressions for electric permittivities in cloaks with non-spherical shapes. This is followed by Sec. 3, in which we numerically clarify their universality concerning the ANEP, and calculate cloaking efficiency under various conditions. This paper ends with a discussion and conclusion in Sec. 4.

2 Formalism

To proceed, we shall use a first-principles approach, namely, the coordinate transformation method.[3−4] We consider that each point in the original orthogonal Cartesian coordinates can be represented as (x, y, z), while in

*Supported by the National Natural Science Foundation of China under Grant Nos. 10604014 and 10874025, by the Shanghai Education Committee and the Shanghai Education Development Foundation ("Shu Guang" Project under Grant No. 05SG01), by the Scientific Research Foundation for the Returned Overseas Chinese Scholars, State Education Ministry, China, and by Chinese National Key Basic Research Special Fund under Grant No. 2006CB921706

†Corresponding author, E-mail: jphuang@fudan.edu.cn

the distorted coordinates it can be given as (u, v, w), which is the location of the new point with respect to the x, y, and z axes, namely, $u = u(x, y, z)$, $v = v(x, y, z)$, and $w = w(x, y, z)$.[3] In the distorted coordinates, the form of Maxwell's Equations are invariant, but the corresponding electric permittivity are got in the following form $\epsilon'_u = \epsilon_u(Q_u Q_v Q_w/Q_u^2)$ (ϵ_u: electric permittivity in the original Cartesian coordinates), where

$$Q_u^2 = \left(\frac{\partial x}{\partial u}\right)^2 + \left(\frac{\partial y}{\partial u}\right)^2 + \left(\frac{\partial z}{\partial u}\right)^2, \tag{1}$$

$$Q_v^2 = \left(\frac{\partial x}{\partial v}\right)^2 + \left(\frac{\partial y}{\partial v}\right)^2 + \left(\frac{\partial z}{\partial v}\right)^2, \tag{2}$$

$$Q_w^2 = \left(\frac{\partial x}{\partial w}\right)^2 + \left(\frac{\partial y}{\partial w}\right)^2 + \left(\frac{\partial z}{\partial w}\right)^2. \tag{3}$$

Now we consider an ellipsoidal cloak in three dimensions. In the Cartesian coordinates (x, y, z), the equation for describing an ellpsoidal shape is

$$\frac{x^2}{a^2} + \frac{y^2}{b^2} + \frac{z^2}{c^2} = 1\,,$$

where a, b, and c are the three principal semi-axes of the ellipsoid, respectively. Next, we choose (λ, μ, ν) to represent a point in the orthogonal ellipsoidal coordinates. So far, the relation between (λ, μ, ν) and (x, y, z) is given as

$$x^2 = \frac{(a^2+\lambda)(a^2+\mu)(a^2+\nu)}{(a^2-b^2)(a^2-c^2)}\,, \tag{4}$$

$$y^2 = \frac{(b^2+\lambda)(b^2+\mu)(b^2+\nu)}{(b^2-c^2)(b^2-a^2)}\,, \tag{5}$$

$$z^2 = \frac{(c^2+\lambda)(c^2+\mu)(c^2+\nu)}{(c^2-a^2)(c^2-b^2)}\,. \tag{6}$$

Then, we squeeze the ellipsoidal volume into an ellipsoidal shell through the following relations

$$\lambda' = a_1 + \lambda\frac{a_2 - a_1}{a_2}\,, \tag{7}$$

$$\mu' = b_1 + \mu\frac{b_2 - b_1}{b_2}\,, \tag{8}$$

$$\nu' = c_1 + \nu\frac{c_2 - c_1}{c_2}\,, \tag{9}$$

where a_1, b_1, and c_1 (a_2, b_2, and c_2) are the inner (outer) three principal semi-axes of the ellipsoidal shell. In the distorted ellipsoidal coordinates, we have the renormalized values of electric permittivities, $\epsilon'_{\lambda'}$, $\epsilon'_{\mu'}$, and $\epsilon'_{\nu'}$, inside the ellipsoidal cloak (shell):

$$\epsilon'_{\lambda'} = \frac{a_2}{a_2-a_1}\frac{b_2}{b_2-b_1}\frac{c_2}{c_2-c_1}\frac{(\lambda'-a_1)^2}{\lambda'^2}\epsilon_{\rm host}\,, \tag{10}$$

$$\epsilon'_{\mu'} = \frac{a_2}{a_2-a_1}\frac{b_2}{b_2-b_1}\frac{c_2}{c_2-c_1}\frac{(\mu'-b_1)^2}{\mu'^2}\epsilon_{\rm host}\,, \tag{11}$$

$$\epsilon'_{\nu'} = \frac{a_2}{a_2-a_1}\frac{b_2}{b_2-b_1}\frac{c_2}{c_2-c_1}\frac{(\nu'-c_1)^2}{\nu'^2}\epsilon_{\rm host}\,, \tag{12}$$

where $\epsilon_{\rm host}$ denotes the electric permittivity outside the cloak. From Eqs. (10)–(12), we can see that the electric permittivities are both materially anisotropic and spatially inhomegeneous in the distorted ellipsoidal coordinates. For achieving them, metamaterials can help.[6] On the other hand, Eqs. (10)–(12) also imply that the gradation of materials offers an additional control to obtain novel cloaking materials, similar to its known role in achieving enhanced nonlinear optical materials.[26−28]

3 Numerical Results

3.1 *Negative Pathway of Electric Displacement Fields*

By using the commercial software COMSOL Multiphysics 3.5 (which is based on the finite element method), we perform the numerical simulations. There are three geometrical regions in the whole system, namely, the inner region (region I), the cloak or shell region (region II), and the outer region (region III), see Fig. 1. For convenience, we set the electric permittivity of region I to have the same value as that $\epsilon_{\rm host}$ of region III, and further take $\epsilon_{\rm host}$ to be equal to the electric permittivity of free space ϵ_0. This will not affect our results at all because the main interest of this work is on geometrical control of electric fields within region II. The electric permittivity of region II is determined according to Eqs. (10)–(12). For all the spherical or non-spherical cloaks discussed in this work, we keep the volume ratio between region II and region I at 7:1, and the applied electric potentials are set to be +3 V and −3 V at the two opposite planes of the cubic box, respectively.

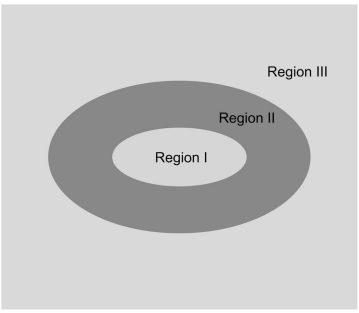

Fig. 1 Schematic graph showing three regions used in our simulations: The inner region (region I), the cloak or shell region (region II), and the outer region (region III).

It is worth mentioning that our results are independent of the actual value of the potentials. As the spherical cloak is centro-symmetric, it makes no difference when the electric field is applied in various directions. However, for an ellipsoidal cloak, we have to discriminate the direction of applied electric fields due to the existence of geometric anisotropy. In our simulations, we apply the electric potentials in two opposite planes along the three principal axes, a, b, and c, of the ellipsoidal cloak, respectively. We focus on two types of rotational ellipsoid (namely, spheroid) with $a < b = c$ (oblate spheroid) and $a > b = c$ (prolate spheroid). Throughout this work, the set of a, b, and c will be used to denote both three inner principal semi-axes (a_1, b_1, and c_1) and three outer principal semi-axes (a_2, b_2, and c_2) of the ellipsoidal cloak if

there are no special instructions. We should also remark that our simulation results are independent of the length scale of the cloaks.

Furthermore, we consider the effect of loss in these cloaks. Throughout this work, we take the loss factor to be $10i$ for model calculations. That is, the factor $10i$ is added to the permittivity of the materials (which make the cloak) as its imaginary part. In fact, if the loss factor is smaller than i, the results we obtain are almost the same as the cases without loss.

The streamlines of Fig. 2(a) represent the pathway of the electric displacement field in the spherical cloak for the parameters as indicated in the caption. Clearly, the displacement field goes around the inner region, but is limited within the cloak (shell), and eventually returns to its original pathway. In this process, an object inside the inner regions has no effect on the electric displacement field at all. In other words, the object is protected from the invasion of electric fields by using the cloak. Figure 2(b) is the cross section of the spherical cloak.

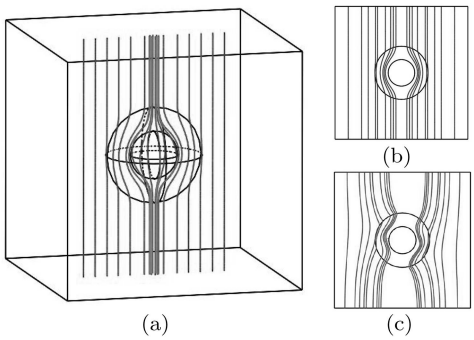

Fig. 2 Spherical cloak without loss (Fig. 2(a)), cross section of the spherical cloak without loss (Fig. 2(b)) and cross section of the spherical cloak with loss (Fig. 2(c)). The streamlines denote the pathway of the electric displacement field when the applied electric potentials are set to be +3 V and −3 V at the top and bottom plane of the cubic box, respectively. Parameters: $r_1 = 0.1$ m (inner radius) and $r_2 = 0.2$ m (outer radius).

For a spheroidal cloak, the pathway of the electric displacement field is also illustrated in Figs. 3(a)–3(b) (oblate spheroid) and Figs. 4(a)–4(b) (prolate spheroid). For the oblate spheroidal cloak $a < b = c$, the pathway is similar to the spherical cloak discussed in Figs. 2(a)–2(b) when the applied electric field is directed along the short principal semi-axis a, see Figs. 3(a)–3(b). However, the situation becomes different for the case of prolate spheroid with $a > b = c$, as shown in Figs. 4(a)–4(b) in which the external electric field is along the long principal semi-axis a. Figures 4(a)–4(b) show an negative pathway of the electric displacement field inside the spheroidal cloak. Here, we called it negative electric polarization (NEP), which means that the displacement field goes backwards, in contrast to normal pathway for which the field goes forwards. (All the NEP streamlines shown in Figs. 4(a)–4(b) are seemingly limited to enter the inner region. However, this is actually not true. Depending on different streamlines/pathways and/or shape parameters, such NEP streamlines can also appear within the cloak region only.) Owing to the symmetry of the prolate spheroid, the NEP zone is strictly symmetrical, which locates close to the two opposite sides of the prolate cloak.

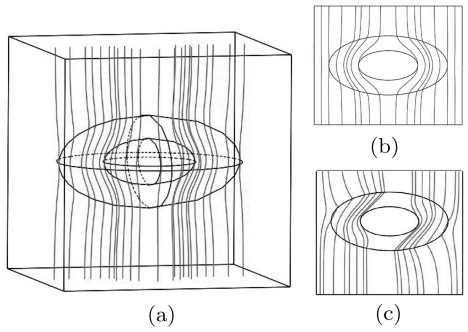

Fig. 3 Oblate spheroidal cloak without loss with three principal semi-axes a, b, and c satisfying $a < b = c$ (Fig. 3(a)), cross section of the oblate cloak without loss (Fig. 3(b)), and cross section of the oblate cloak with loss (Fig. 3(c)). The streamlines denote the pathway of the electric displacement field in the direction of the short axis a when the applied electric potentials are set to be +3 V and −3 V at the top and bottom plane of the cubic box. Parameters: $a_1 = 0.1$ m and $b_1 = c_1 = 0.2$ m (three inner principal semi-axes); $a_2 = 0.2$ m, and $b_2 = c_2 = 0.4$ m (three outer principal semi-axes).

On the other hand, we have also investigated the case of a general ellipsoid with $a \neq b \neq c$ for which the external electric field is directed along the longest principal semi-axis, the behavior is generally similar to Figs. 4(a)–4(b) (no figures shown here). For the ellipsoidal cloak, we consider the electric displacement field along the three principal axes, in contrast to that along two principal axes of spheroidal or elliptical cloaks. As an incident electric field is directed along the long (or longest) principal axis, the behavior of 2D elliptical (or 3D ellipsoidal cloaks) is similar to Fig. 4 for 3D spheroidal cloaks. Otherwise, their appearance looks similar to Fig. 3. Nevertheless, in this case, the NEP zone is no longer strictly symmetrical, the degree of which depends on the actual values of a, b, and c.

When the effect of loss (loss factor: $10i$) is considered, the corresponding pathway of the electric displacement field is displayed in Fig. 2(c), Fig. 3(c), and Fig. 4(c), respectively. Apparently, the behavior is very different from that for the cases without loss. Nevertheless, we should stress that all the general results obtained from Figs. 2(a)–2(b), Figs. 3(a)–3(b), and Figs. 4(a)–4(b) can also work for the cases with loss as long as the loss factor is smaller than i for the current parameters in use.

In the prolate spheroidal cloak, the displacement field displays a pathway that is inverse to the external electric field (Figs. 4(a)–4(b)), thus indicating the appearance

of apparently negative polarization. As for the spherical cloak, the electric displacement field goes around the inner geometrical region as if there is nothing in it (Figs. 2(a)–2(b)), and the streamlines show no inverse pathway. Thus, the NEP does not occur for a spherical cloak. Now let us explain the NEP in more details. In a model NEP line, see Fig. 5, the electric displacement goes from the top to the bottom. First let us take two points A and B along the displacement field, the potential U_A at A must be larger than that U_B at B according to the fundamental knowledge of electrodynamics. However, in the simulation the top side has a higher potential than the bottom side in this reverse region. In other words, U_B is apparently higher than U_A in the simulation. Thus, we conclude that the NEP line corresponds to an area with ANEP (apparently negative electric polarization). Here we want to stress one point, NEP is a general phenomena which can happen in many cases, while ANEP is a special case of the NEP in the study here. Explicitly speaking, NEP is just ANEP throughout this work. So far, we may conclude that the appearance of the ANEP zone is driven by geometrical shapes.

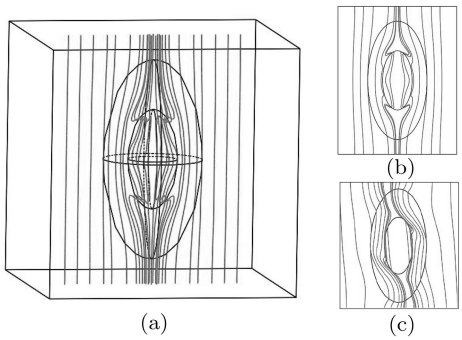

Fig. 4 The same as Fig. 3, but for prolate spheroidal cloak $a > b = c$ and the electric displacement field in the direction of the long axis a. Parameters: $a_1 = 0.2$ m and $b_1 = c_1 = 0.1$ m; $a_2 = 0.4$ m, and $b_2 = c_2 = 0.2$ m.

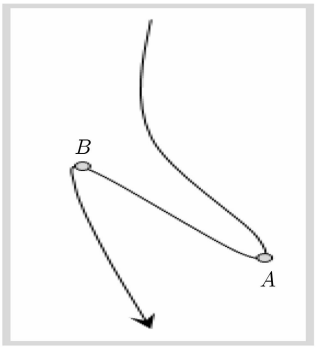

Fig. 5 Schematic graph showing the trajectory of a displacement field. The arrow indicates the direction of the field. The line AB denotes an NEP (or ANEP) line.

For spheroidal cloak with three principal semi-axes $a \neq b = c$, in the presence of external electric fields along the direction of the principal semi-axis a, Fig. 6(a) shows the potential difference U_{AB} as a function of the ratio between a and b ($a : b$) ranging from 0 to 3.6. When the ratio is larger than 1, the potential difference U_{AB} will increase as a function of the ratio. To understand more clearly, in Fig. 6(b) we investigate U_{AB} as a function of $a : b$ ranging from 0 to 20. It is evident that when $a : b$ is smaller than or equal to 1 (oblate spheroid or sphere), the electric potential $U_{AB} = 0$, namely, there is no ANEP. As $a : b > 1$ (prolate spheroid), the ANEP comes to appear, and reach maximum at about $a : b = 5 : 2$. Eventually, it tends to disappear as $a : b$ is large enough corresponding to a rod-like shape.

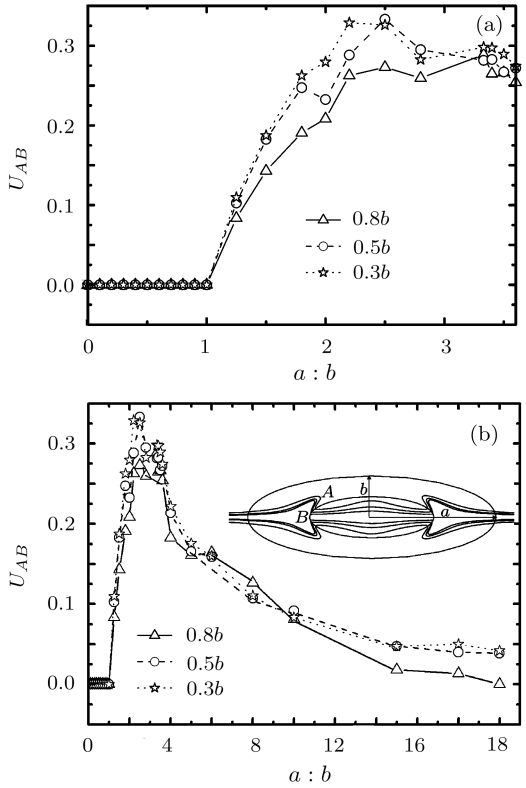

Fig. 6 (a) The potential difference U_{AB} between the starting point A and ending point B of the ANEP streamline [as also indicated in the inset of (b)] is a function of the ratio between a and b ($a : b$) ranging from 0 to 3.6. The three curves correspond to the three incident electric fields, which respectively have a vertical distance of $0.8b$, $0.5b$, and $0.3b$ with respect to the principal semi-axis a, see also the inset of (b). (b) U_{AB} as a function of $a : b$ ranging from 0 to 20, and others are the same as (a).

Figure 7 illustrates the paired electric permittivities, ϵ_λ and ϵ_μ, in the ANEP streamline within the cross section of the spheroidal cloak with $a > b = c$ as a function of the distance r (see the caption), for $a : b =$ (a) 2 : 1, (b) 3 : 1, and (c) 4 : 1. The permittivity components shown in Eqs. (10)–(12) are functions of the position in the transformed coordinates. All the points displayed in Figs. 7(a)–7(c) have been taken in sequence from the starting point to the ending point of the ANEP streamline, as indicated by the ordered numbers. As $a : b$ is given, all

the paired ε_λ and ε_μ (corresponding to the same number) appear in a symmetric oscillation trajectory, and satisfy a sum rule: (a) $\varepsilon_\lambda + \varepsilon_\mu = 2.015 \pm 0.003$, (b) 2.218 ± 0.007, and (c) 2.461 ± 0.006. It is worth noting that the electric permittivity ε_ν keeps unchanged for the cross section (in two dimensions) of our interest.

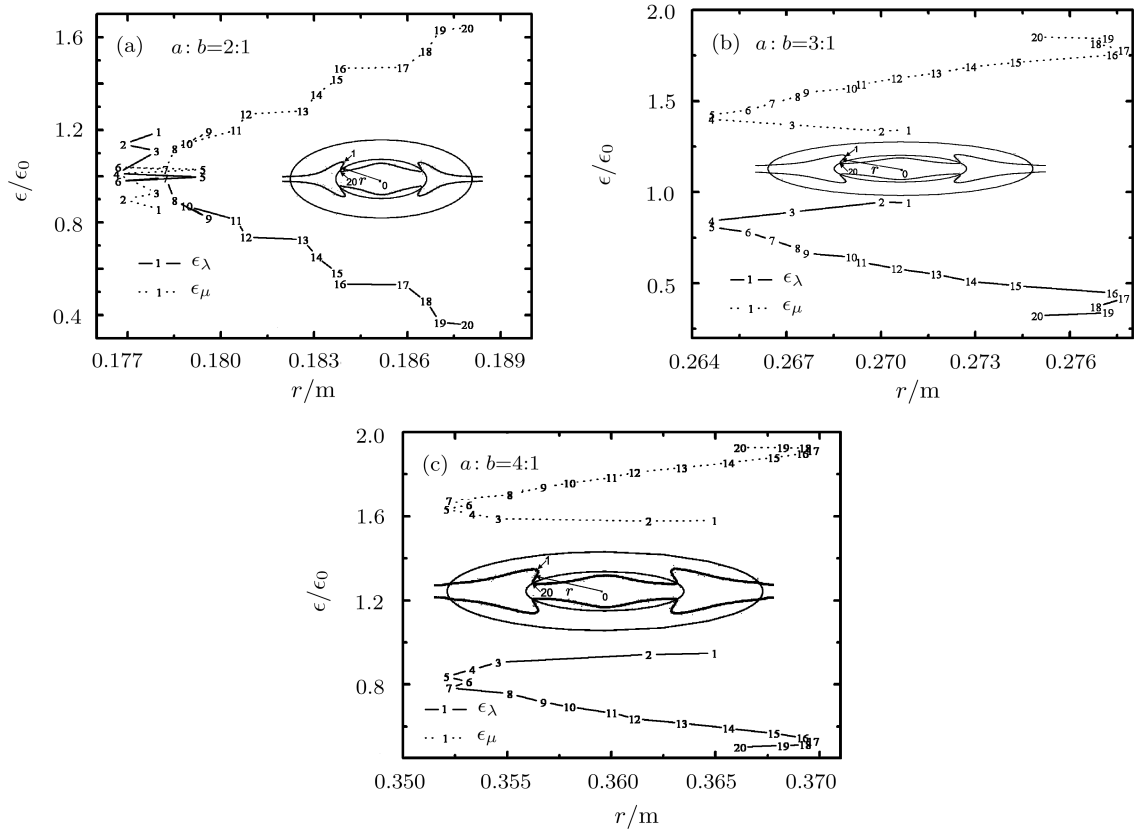

Fig. 7 The paired electric permittivities, ϵ_λ and ϵ_μ, in the ANEP streamline within the cross section of the spheroidal cloak without loss with $a > b = c$ as a function of the distance r between any point in the ANEP streamline and the center of the cloak, for (a) $a : b = 2 : 1$, (b) $a : b = 3 : 1$, and (c) $a : b = 4 : 1$. All the 20 points have been taken in sequence from the starting point to the ending point of the ANEP streamline, as clearly indicated in the corresponding ordered numbers, see also the three insets.

3.2 *Cloaking Efficiency*

For the cloaks of our interest, we adopt a convenient definition based on the concept of electric energy. That is, we define the cloaking efficiency η as the ratio between the total electric energy of geometrical regions II and III and that of the whole system of regions I, II, and III. Apparently, if η is equal to 100%, the cloaking is perfect. In this case, any objects within region I can be perfectly shielded from external electric fields. In other words, the degree of imperfectness of the cloaking is denoted by how η deviates from 100%.

For consistence, the applied electric potentials and the electric permittivities of geometrical regions I, II, and III are set to be the same as those already presented in the previous section. In the simulations, the volume ratio between region II and region I is also kept at 7:1.

The calculated cloaking efficiencies of the cloaks without loss under different conditions are shown in Tables 1–3. As we can see, the cloaking efficiency of the spherical cloak is 99.58%, which is very close to, but not equal to 100% (perfect cloaking). The deviation from 100% arises from the small amount of central streamlines that unavoidably pass through region I. Further, we find that the cloaking efficiencies of non-spherical cloaks are always smaller than that of the spherical cloak. In detail, for prolate spheroidal ($a > b = c$), oblate spheroidal ($a < b = c$), and ellipsoidal ($a \neq b \neq c$) cloaks, their cloaking efficiencies corresponding to three different principal semi-axes have only slight difference and are smaller than that of the spherical cloak. For the three kinds of non-spherical cloaks, we can conclude that the cloaking efficiency corresponding to the field directed along the longest principal semi-axes is the smallest among those along the three principal semi-axes, and that the cloaking efficiency of ellipsoidal ($a \neq b \neq c$) cloaks is the largest whereas that of oblate spheroidal ($a < b = c$) cloaks is the smallest. Also evidently, Tables 1–3 have numerically shown that the cloak with ANEP has a lowest cloaking efficiency, see $\eta = 99.14\%$ in Table 1, $\eta = 97.69\%$ in Table 2, and $\eta = 99.52\%$ in Table 3.

Table 1 Cloaking efficiency η of spherical and prolate spheroidal ($a > b = c$) cloaks without loss. The external DC electric field is applied along the a, b, and c principal semi-axes, respectively. r_1 (or r_2) denotes the inner (or outer) radius of a spherical cloak.

Shape	Direction	Inner	Outer	η
Sphere		$r_1 = 0.1$ m	$r_2 = 0.2$ m	99.58%
Spheroid	a	$a_1 = 0.2$ m, $b_1 = 0.1$ m, $c_1 = 0.1$ m	$a_2 = 0.4$ m, $b_2 = 0.2$ m, $c_2 = 0.2$ m	99.14%
Spheroid	b or c	$a_1 = 0.2$ m, $b_1 = 0.1$ m, $c_1 = 0.1$ m	$a_2 = 0.4$ m, $b_2 = 0.2$ m, $c_2 = 0.2$ m	99.15%

Table 2 Cloaking efficiency η of oblate spheroidal ($a < b = c$) cloaks without loss.

Shape	Direction	Inner	Outer	η
Spheroid	a	$a_1 = 0.1$ m, $b_1 = 0.2$ m, $c_1 = 0.2$ m	$a_2 = 0.2$ m, $b_2 = 0.4$ m, $c_2 = 0.4$ m	97.75%
Spheroid	b or c	$a_1 = 0.1$ m, $b_1 = 0.2$ m, $c_1 = 0.2$ m	$a_2 = 0.2$ m, $b_2 = 0.4$ m, $c_2 = 0.4$ m	97.69%

Table 3 Cloaking efficiency η of ellipsoidal ($a \neq b \neq c$) cloaks without loss.

Shape	Direction	Inner	Outer	η
Ellipsoid	a	$a_1 = 0.1$ m, $b_1 = 0.2$ m, $c_1 = 0.4$ m	$a_2 = 0.2$ m, $b_2 = 0.4$ m, $c_2 = 0.8$ m	99.55%
Ellipsoid	b	$a_1 = 0.1$ m, $b_1 = 0.2$ m, $c_1 = 0.4$ m	$a_2 = 0.2$ m, $b_2 = 0.4$ m, $c_2 = 0.8$ m	99.56%
Ellipsoid	c	$a_1 = 0.1$ m, $b_1 = 0.2$ m, $c_1 = 0.4$ m	$a_2 = 0.2$ m, $b_2 = 0.4$ m, $c_2 = 0.8$ m	99.52%

As a matter of fact, our qualitative results are independent of the explicit value of the volume ratio. For instance, we set the ratio to be 19:8, and plot the pathway of the electric displacement field (no figures shown here). The efficiency has little difference. Clearly, for different volume ratios, the efficiency of cloaking is unchanged for spherical cloaks, and only varies slightly for non-spherical cloaks. In general, all the above qualitative results remain the same for difference volume ratios.

On the other hand, from Table 4, we find that for cloaks with loss, the efficiency of cloaking is reduced slightly in comparison with those without loss. Nevertheless, for spherical cloaks, the efficiency keeps unchanged no matter whether there exists the loss or not.

Table 4 Cloaking efficiency η of cloaks with loss or without loss, for the three structures displayed in Figs. 1, 2, and 3, respectively.

	Fig. 1	Fig. 2	Fig. 3
Without loss	$\eta = 0.9658$	$\eta = 0.9341$	$\eta = 0.9357$
With loss	$\eta = 0.9658$	$\eta = 0.9111$	$\eta = 0.9028$

4 Discussion and Conclusion

Besides DC electric fields adopted in the above simulations, our results also hold for AC fields due to the symmetry of the system. Since they have been obtained by using numerical simulations according to a first-principles approach, namely, the coordinate transformation method, they are exact without any approximation (despite the error which might occur when we extracted the data, e.g., as implied by the sum rules obtained from Fig. 7).

Regarding an experimental demonstration, it would be quite convenient to use metamaterials to realize the cloaks with a shape-driven negative electric polarization, due to the existing significant achievements in the field.[5−6] Further, the fact that our results do not depend on specific length-scales makes the experiment more tractable. For the applications, the negative polarization region has relevance to dielectric shielding and the energy conservation. Actually it has been studied in many other areas such as the quantum system to realize the quantum repeater with a long spin memory time[29−30] and the ferroelectrics to have a short switching time.[31]

For the cloaks of our interest, based on the concept of electric energy, we have defined the cloaking efficiency η as the ratio between the total electric energy of geometrical regions II and III and that of the whole system of regions I, II, and III. On the other hand, for general electromagnetic cloaks, one has used "scattering efficiency" to represent the efficiency of cloaking.[32] While the definition of "scattering efficiency" was adopted according to the Mie theory for general electromagnetic waves, our definition is for DC (or AC) electric fields according to the finite element method, and thus should also be accurate and precise.

To sum up, we have accurately revealed the universality concerning a class of shape-dependent ANEP in shaped graded dielectric materials existing in the form of cloaks with various shapes. Under certain circumstances the streamlines of the electric displacement field may partly loop backwards. And it arises from a symmetric oscillation of the paired electric permittivities, which have been demonstrated to satisfy a sum rule. The cloaking efficiency has further been calculated for various geometrical shapes, and demonstrated to be closely related to the ANEP.

References

[1] V.G. Veselago, Soviet Physics USPEKI **10** (1968) 509.

[2] J.B. Pendry, A.J. Holden, W.J. Stewart, and I. Youngs, Phys. Rev. Lett. **76** (1996) 4773.

[3] J.B. Pendry, D. Schurig, and D.R. Smith, Science **312** (2006) 1780.

[4] D. Schurig, J.B. Pendry, and D.R. Smith, Opt. Express **14** (2006) 9794.

[5] D. Schurig, J.J. Mock, B.J. Justice, S.A. Cummer, J.B. Pendry, A.F. Starr, and D.R. Smith, Science **314** (2006) 977.

[6] D.R. Smith, J.B. Pendry, and M.C.K. Wiltshire, Science **305** (2004) 788.

[7] H. Chen, B. Wu, B. Zhang, and J.A. Kong, Phys. Rev. Lett. **99** (2007) 063903.

[8] H. Chen and C.T. Chan, J. Appl. Phys. **104** (2008) 033113.

[9] W. Cai, U.K. Chettiar, A.V. Kildishev, and V.M. Shalaev, Nature Photonics **1** (2007) 224.

[10] F. Zolla, S. Guenneau, A. Nicolet, and J.B. Pendry, Opt. Lett. **32** (2007) 1069.

[11] H.Y. Chen and C.T. Chan, Appl. Phys. Lett. **90** (2007) 241105.

[12] U. Leonhardt, New J. Phys. **8** (2006) 118.

[13] G.W. Milton and N.A.P. Nicorovici, Proc. R. Soc. A **462** (2006) 3027.

[14] L.H. Shi, L. Gao, S.L. He, and B.W. Li, Phys. Rev. B **76** (2007) 045116.

[15] W.T. Dong and L. Gao, J. Appl. Phys. **104** (2008) 023537.

[16] O.P. Brunoa and S. Lintner, J. Appl. Phys. **102** (2007) 124502.

[17] A. Nicolet, F. Zolla, and S. Guenneau, IEEE Trans. Magn. **44** (2008) 1150.

[18] H. Ma, S. Qu, Z. Xu, J. Zhang, B, Chen, and J. Wang, Phys. Rev. A **77** (2008) 013825.

[19] D.H. Kwon and D.H. Werner, Appl. Phys. Lett. **92** (2008) 013505.

[20] S.A. Cummer and D. Schurig, New J. Phys. **9** (2007) 45.

[21] B. Liu and J.P. Huang, Eur. Phys. J. Appl. Phys. **48** (2009) 20501.

[22] B. Liu and J.P. Huang, Commun. Theor. Phys. **53** (2010) 560.

[23] G.W. Milton, M. Briane, and J.R. Willis, New J. Phys. **8** (2006) 248.

[24] Y. Cheng and X.J. Liu, J. Appl. Phys. **104** (2008) 104911.

[25] C.Z. Fan, Y. Gao, and J.P. Huang, Appl. Phys. Lett. **92** (2008) 251907.

[26] J.P. Huang and K.W. Yu, Phys. Rep. **431** (2006) 87.

[27] L. Gao and X.P. Yu, Eur. Phys. J. B **55** (2007) 403.

[28] J.P. Huang, L. Gao, and Z.Y. Li, Commun. Theor. Phys. **36** (2001) 251.

[29] M.L. Reed, E.D. Readinger, C.G. Moe, H. Shen, M. Wraback, A. Syrkin, A. Usikov, O.V. Kovalenkov, and V.A. Dmitriev, Phys. Status Solidi C **6** (2009) 585.

[30] H. Kosaka, Y. Rikitake, H. Imamura, Y. Mitsumori, and K. Edamatsu http://arxiv.org/abs/quant-ph/0609152.

[31] J. Li, B. Nagaraj, H. Liang, W. Cao, Chi.H. Lee, and R. Ramesh, Appl. Phys. Lett. **84** (2004) 1174.

[32] A. Alu and N. Engheta, Phys. Rev. Lett. **100** (2008) 113901.